Elastic Strain of PTT/PET Self-Crimping Fibers

Fumei Wang, PhD[1], Fei Gu[1], Bugao Xu, PhD[2]

[1]College of Textiles, Donghua University, Shanghai CHINA

[2]University of Texas, Austin, Texas UNITED STATES

Correspondence to:
Fumei Wang email: wfumei@dhu.edu.cn

ABSTRACT

This paper studies the relationship between crimp curvatures and elastic strains of two series of PTT (Polytrimethylene terephthalate)/ PET (Polyethylene terephthalate) self-crimping fibers produced with two different spinnerets which merge PTT and PET fluids at different points. The crimp curvature is estimated based on fiber cross-sectional parameters and the polymer properties. The elastic strain, the strain associated with crimp removal, is measured directly from the stress-strain curves of the fibers. It was found that the crimp curvatures of the PTT/PET filaments in the two series increased with their PTT contents. The elastic strains of the PTT/PET filaments in each series showed a linear positive correlation with the estimated crimp curvatures. A linear equation (R=0.979) was established to predict the elastic stain from the calculated curvature for fibers in different series. This prediction equation can help to determine appropriate fiber cross section, composite ratio and distribution of the two components in the design stage of filament. The paper also shows a color image of dyed PTT/PET filaments, which is helpful in examining the interfacial morphology of the two components. Thus, the spinning method has a certain influence on the interfacial morphology of the fiber cross-section.

Keywords: PTT/PET self-crimping fiber, elastic strain, crimp curvature, interface morphology.

INTRODUCTION

PTT/PET filament is a bicomponent fiber made of PTT and PET materials by compound spinning. Due to differences in thermal shrinkage and modulus of the two components, the filament is naturally crimped in high frequency, helical fluctuations after the spinning and downing process, which provides excellent lasting elasticity for fabrics [1-10]. Elastic elongation and recovery rate are the two main parameters used to characterize the elasticity. The elongation of PTT/PET self-crimping filament includes crimp extension and material elongation, and the former is the dominant constituent in the total elongation. It is useful to know the potential elastic properties in the filament design and development stage. Theoretical crimp modeling of side-by-side bicomponent fibers has been explored to predict crimp curvature and elastic moduli [6,11]. It is important to further study the relationship between the theoretical calculated curvature of PTT/PET self crimping filaments and the measured elastic elongation, in order to predict the elastic elongation of PTT/PET self crimping fibers.

EXPERIMENTAL

Samples

Six PTT/PET self-crimping filament samples used in the experiment are shown in *Table I*. The samples can be divided into two series according to the spinnerets used. For filaments in series B, two polymer fluids were merged within the spinneret, and are extruded from the same orifice. For filaments in series K, two polymer fluids were extruded separately through two adjacent orifices, and were immediately bonded together after spinning. In each series, three kinds of filaments were produced by changing the component ratio. Except for the spinneret and the component ratio, other spinning and drawing conditions of the six samples were identical. The intrinsic viscosities of PTT and PET are 1.3 dL/g and 0.64 dL/g, respectively. The linear density of filaments in the six samples is 111dtex/24f.

TABLE I. PTT/PET self-crimping filaments.

Series	Sample	Spinneret	PTT/PET ratio
B	B1	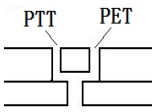	50/50
	B2		60/40
	B3		40/60
K	K1	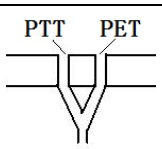	50/50
	K2		60/40
	K3		40/60

PTT/PET filaments gain full crimp only after stress relaxation. In order to make filaments retain crimp in finished fabrics, the filaments need to be set using a heat set treatment method [7]. In this experiment, 20 filament specimens were randomly cut into 1-meter length from each sample, and were treated in an electrically-heated water bath pot at 100 ℃ for 15 minutes. The specimens were then removed the for natural drying, and conditioned in the standard testing environment (temperature 20 ± 2℃, relative humidity 65% ± 5%) for 24 hours.

Elastic Strains of PTT/PET Self-Crimping Fibers

The stress-strain curves of the treated filaments were tested with an XN-1 type elastic yarn tester at a gauge length of 50 mm, drawing speed of 500 mm/min (CRE), and pre-tension of 0.01±0.001 cN/dtex. *Figure 1* shows a typical stress-strain curve of the specimens, on which O is the starting point and B is the breaking point. The entire strain can be divided into two sections: OA—crimp strain and AB—fiber strain. OA indicates the extension that straightens crimp under a small tensile force, and is named as the elastic strain since it can be recovered once the stress is removed. Compared to AB, OA is a much larger deformation. Since the multifilament yarn is networked at discrete points, and the filaments are not completely parallel, a few small fluctuations appear on section AB. In order to measure the elastic strain (OA), point A must be suitably selected. On the stress-strain curve, one can draw a line connecting points O and B, and then draw a tangent line which is parallel to OB. The tangent point can be used as point A.

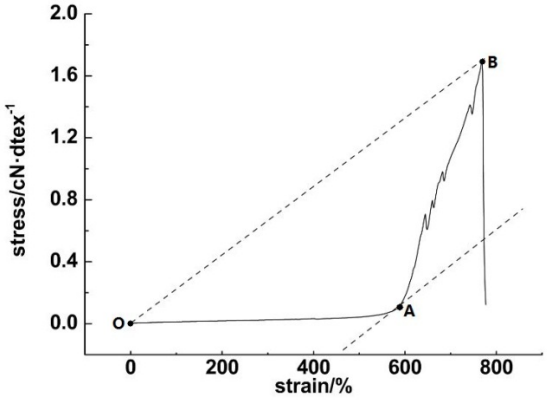

FIGURE 1. Stress-strain curve of sample B2.

A total of 120 stress-strain curves for the six samples were analyzed by using the above method. The averages and coefficients of variation (CV) of the elastic strains are shown on *Table II*. The three samples in series B have much larger elastic strains than those in series K. The elastic strain of the PTT/PET self-crimping filament increases in both series as the PTT content increases, although series B has much higher increase rates than series K. The CVs of the elastic strains in the both series appear to be at comparable levels in a range of 10% to 20%.

TABLE II. Elastic strain of PTT/PET self-crimping fibers.

Sample	Elastic strain	
	Mean (%)	CV (%)
B3	364.6	15.69
B1	553.1	11.22
B2	583.0	11.12
Mean	500.2	12.68
K3	292.8	9.95
K1	328.3	18.90
K2	389.4	13.61
Mean	336.8	14.15

Curvature for PTT/PET Self-Crimping Filament

Denton [11] derived a curvature calculation equation to characterize the relationship of fiber curvature ρ and the material parameters for self-crimping bicomponent fibers:

$$\rho = \frac{1}{R} = \frac{A_1 A_0 u_2 \Delta}{A_0(I_{1p}+I_{2p})+(m-1)(A_2 I_{2P}-\frac{1}{m}A_1 I_{1P}-\frac{m-1}{m}A_2^2 u_2^2)} \quad (1)$$

where R is the radius of a crimp curve; m is the ratio of elastic modulus of the two components ($m = E_2/E_1$); $\triangle$ is the difference of thermal shrinkage ratios between the two components; A_1 and A_2 are the areas of the fiber cross section respectively occupied by the two component materials, A_0 is the total fiber cross-sectional area ($A_0 = A_1+A_2$); u_1 and u_2 are the distances from the centroids of the two component areas to the centroid of the fiber cross section, respectively; I_1 and I_2 are the moments of inertia of the two sections around the axes through their own centroids, and I_{1P} and I_{2P}, are the moments of their inertia relative to the axis through the fiber centroid ($I_{1P}=I_1+A_1u_1^2$ and $I_{2P}=I_2+A_2u_2^2$). For most of the commercial PTT/PET bicomponent fibers, Δ and m are known (averagely, $\Delta = 0.0853$, $m = 0.333$)[6]. With these two parameters and the geometrical information measured from the fiber cross-section, one can estimate the possible fiber curvature ρ using Eq. (1).

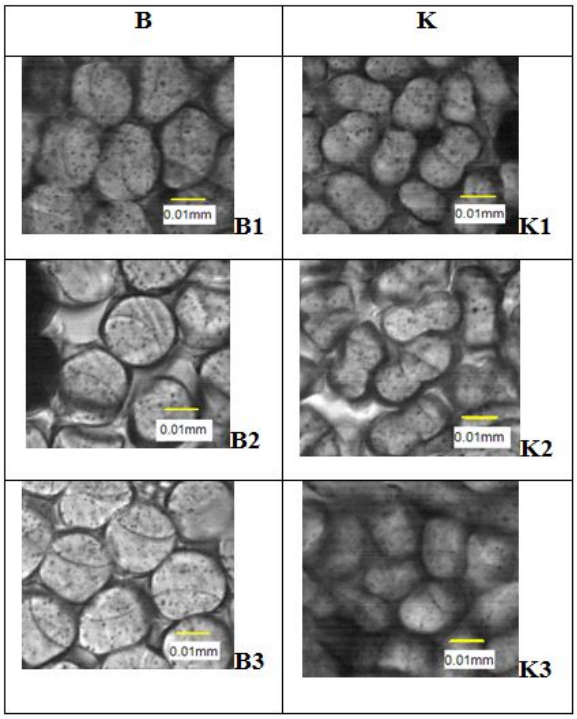

FIGURE 2. Cross-section of PTT/PET self-crimping fibers.

Figure 2 displays the cross-sections of the six PTT/PET fibers, whose shapes vary from circular (B series), to dumbbell (K series). Due to fluctuations in cooling conditions, cross-section shapes of fibers in one series also varied slightly. Dividing lines of the PTT and PET materials are visible on some of the cross sections in the images. Ideally, these images should be processed automatically by image analysis software to obtain geometrical information needed for calculating the centroids for the component and the fiber. Since many fibers in an image intercept or overlap each other, correct image segmentation and fiber separations are extremely difficult in an unsupervised manner. We would have to manually select those cross-sections that have good integrity and representation for fibers in the series for geometrical measurements. *Figure 3* shows one example of the image-processing steps needed for the centroid calculation of a cross section. *Figure 3a* is a fiber cropped from *Figure 2b*. The cropped image was segmented using the adaptive thresholding method [13] (*Figure 3b*). The four corners of the segmented image were filled with black pixels so that the background and the boundary of the cross section were merged (*Figure 3c*). After the removal of the black pixels within the cross section, the contour of the cross section could be extracted with the morphological operations [13] (*Figure 3d*). To locate the separation line of the bicomponents correctly, the operator needed to identify the two endpoints and a few midpoints along the line manually, and our program would form a continuous curve with the B-spline approximation (*Figure 3e*). Once the fiber boundary and the dividing line were extracted, the bicomponent regions can be marked (*Figure 3e*), and the areas (A_1, A_2 and A_0) can be calculated simply by counting pixels in separate regions.

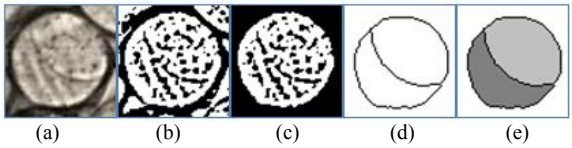

FIGURE 3. Centroid calculation of fiber cross section, (a) Selected cross section, (b) Segmentation, (c) Filled background, (d) Boundary, and (e) Component regions.

The centroid (X, Y) of a region (R) is defined as the average location of the pixels (x_i, y_i) in the region [12], that is,

$$X = \frac{1}{N}\sum_{i\subset R} x_i,\ Y = \frac{1}{N}\sum_{i\subset R} y_i, \quad (2)$$

where N is the number of the pixels in R. Once the centroids of the three regions (two components and fiber cross section) were found, the distances between the centroids, u_1 and u_2, became available.

In order to calculate the inertia moment I of an irregularly shaped region to the centroidal axis, the region can be divided into a series of narrow strips

(*Figure 4*) [12]. Let δ and n be the height and number of the stripes, respectively. If each strip is approximated by a rectangle, the inertia moment of the region can be approximately calculated as follows:

$$I = \delta \sum_{i=1}^{n} a_i^2 b_i \quad (3)$$

where a_i is the distance from the center line of the ith strip to the centroidal axis, and b_i is the mid width of the strip. We calculated I_1 and I_2 for the PTT/PET regions in the cross section using Eq. (3), and estimated the crimp curvatures of the six PTT/PET self-crimping fibers. As show in *Table III*, fiber crimp curvatures increased with PTT contents, but did not change significantly between the two series fibers.

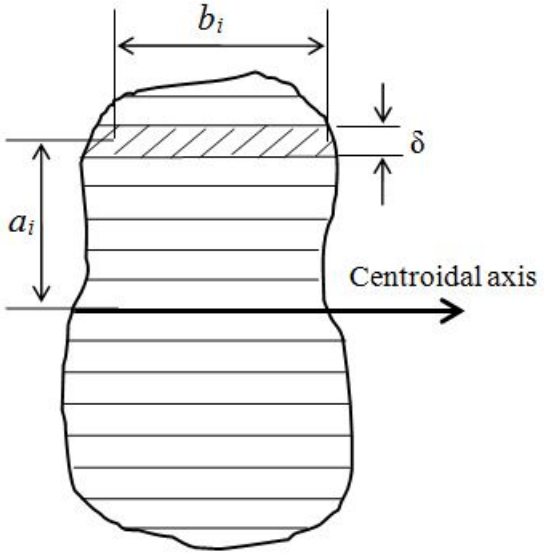

FIGURE 4. Moment of inertia calculation.

TABLE III. Crimp curvature of PTT/PET self-crimping fibers.

Sample No.	PTT area ratio (%)		Curvature ρ(mm^{-1})	
	Mean	CV (%)	Mean	CV (%)
B3	41.1	8.93	5.11	3.90
B1	53.5	6.79	6.15	6.40
B2	59.3	5.36	6.59	8.20
Mean	51.3	7.02	5.95	6.17
K3	38.5	7.03	5.51	7.53
K1	43.5	8.45	6.27	1.18
K2	71.2	13.3	6.38	8.07
Mean	51.0	9.59	6.05	5.59

Relationship Between Elastic Strains and Crimp Curvatures

Figure 5 shows the relationship between the measured elastic strains and the calculated curvatures of the six PTT/PET fibers in B and K series. The vertical coordinate indicates the mean ± standard deviation of 20 measured elastic strains for each fiber, and the horizontal coordinate represents the mean ± standard deviation of 5 calculated curvatures of the corresponding fiber. Using the average values in each series to perform the linear regression, we obtained two best-fitting lines showing the changing trend of elastic strains with curvatures (*Figure 5*). The correlation coefficients of the two regression lines are 0.986 and 0.847, respectively. It is clear that the two parameters are positively correlated. The steeper slope of the fitting line for series B suggests that the curvature of the fibers in series B has more impacts on the elastic strain than those in series K.

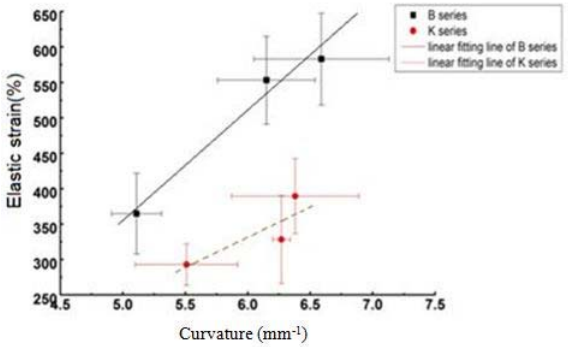

FIGURE 5. Elastic strains and crimp curvatures.

It is also noted that there is a gap between the linear fitting lines of the two series, meaning that the elastic strains of series B is systematically higher than those of series K at given curvatures. This is due to the difference in the filament extrusions of the two series. As introduced before, PTT and PET polymer fluids in series K are extruded separately through their own orifices and then are bonded together. For fibers in series K, two polymer fluids are completely surrounded by cooling air during the time from leaving the spinneret to bonding, and thus can be cooled faster and cured earlier. This leads to a higher orientation and crystallinity of the PTT component in series K [10].

The high orientation and crystallinity of the PTT component in series K make its thermal shrinkage difference ($\triangle_K$) lower than that in series B ($\triangle_B$), i.e., $\triangle_K < \triangle_B$, which in turn lessens curvature and elastic strain of fibers in series K. In addition, the ratio of elastic modulus m of the two components also changes, but its change is lower than that of $\triangle$.

In *Figure 5*, fiber curvatures of the two series were calculated based on an overall Δ value calculated with the fibers in B series[6], ie., Δ= 0.0853, but the two regression lines are distinctly separate. It was pointed out above that in fact $\triangle_k < \triangle_B$, and therefore the relationships between elastic strain and curvature in the two series may be different from those in *Figure 5*. It is necessary to re-estimate $\triangle_k$. Since K2's elastic strain falls with the range of the elastic strains of series B (*Table II*), we may use the regression equation of series B to determine the corresponding curvature of K2 and then further to estimate its thermal shrinkage difference, $\triangle_k$= 0.0699. With this new $\triangle_k$, the curvatures of the other two fibers in series K were re-calculated, and plotted along with the data of series B in *Figure 6*. The data from the two series fibers in *Figure 6* are more linearly correlated (R=0.979), and the best-fitting line may be useful for predicting the elastic strains of PTT/PET self-crimping fibers when the curvature is calculated, that is,

$$\text{Elastic strain (\%)} = 154.85\rho - 426.43 \qquad (4)$$

This prediction equation can help to discover unreasonable fiber cross section, composite ratio and distribution of the two components in the stage of filament design.

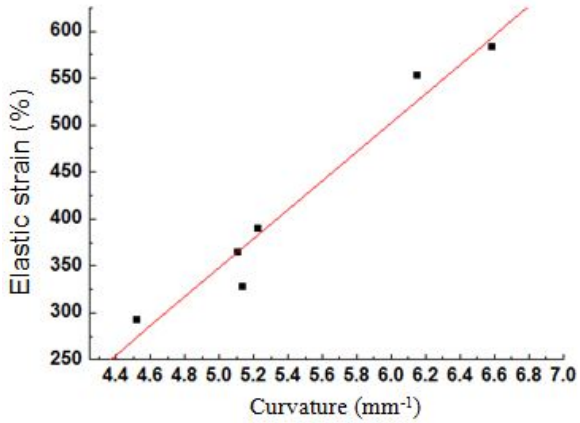

FIGURE 6. Modified relationship of elastic strain and curvature.

Interface Morphology of PTT/PET Components

The shape of a fiber cross section is mainly dictated by the spinneret orifice, but is also affected by the internal stress of the polymer fluids and the external cooling condition when the fluids are rapidly extruded from spinneret holes. To better observe the interface morphology of PTT and PET components in fiber cross sections, we dyed the samples at 100℃. Since PET must be dyed at higher temperature (120~130℃) than PTT, the dye would be mainly distributed in the PTT component, making the regions of the two components more easily differentiated in a color image. *Figure 6* displays the color images of dyed B3 and K2 fibers. It is clear to see that the two component materials are bonded firmly side by side in the fiber cross-section. No separation is found from each other. The interface of the two components in B series fibers is curved towards PTT component. The interface of the two components in K series is relatively straight. Therefore, spinning methods have a certain influence on the interfacial morphology of two components, and the spinning method for K series is easier to form a flat interface.

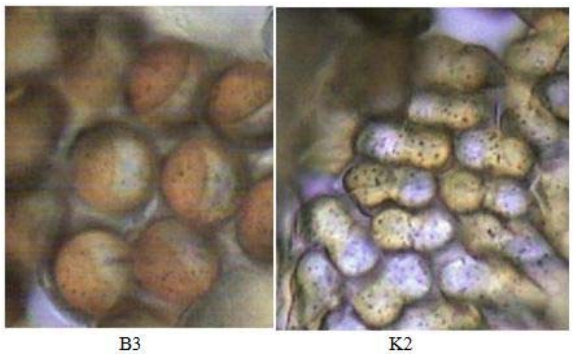

FIGURE 7. Cross sections of dyed fibers.

CONCLUSIONS

The paper demonstrates how to use fiber cross-sectional parameters to estimate crimp curvatures of PTT/PET self-crimping fibers, and studies the impact of fiber crimp curvatures on fiber elastic strains. We found out that the crimp curvature of the PTT/PET fibers in the both series increased with the PTT content, but did not change significantly with different spinnerets (B or K series). The elastic strains of the PTT/PET fibers in each series showed a linear positive correlation with the estimated crimp curvatures. After modifying the thermal shrinkage difference of K series fibers, one linear equation (R=0.979) was established to predict the elastic stain from the calculated curvature for fibers in the both series. This prediction equation can help to determine appropriate fiber cross section, composite ratio and distribution of the two components in the design stage of filament. Color images of dyed PTT/PET fibers were helpful in examining interfacial morphology of the two components. B series fibers seem to have a curved interface between the two components, while K series tends to have a

flat interface. Thus, the time when two polymer fluids begin to merge was found to have a certain influence on the interfacial morphology in fiber cross-section.

ACKNOWLEDGMENTS

The authors gratefully acknowledge the support of the Chinese National Science Foundation (NSFC 50973015).

REFERENCES

[1] Jin Luo, Fumei Wang, Bugao Xu, Elasticity of woven fabrics made of PTT/PET bicomponent filaments. *Textile Research Journal*. Vol.81 (8): 865-870, 2011.

[2] Qian, Y. H., Wang, F. M., and Zhao, L., "Development of PTT Fiber and Product," China Textile Publishing House, Beijing, China, 2006.

[3] Tae H O., Effects of spinning and drawing conditions on the crimp Contraction of side-by-side poly (trimethylene terephthalate) bi-component fibers. Journal of Applied Polymer Science, 102(2):1322-1327, 2006.

[4] RWEI S P, LIN Y T, SU Y Y., Study of self-crimp polyester fibers. Polymer Engineering and Science, 45(6): 838-845, 2005.

[5] Tae, H. O., Melt spinning and drawing process of PET side-by-side composite fibers, Journal of Applied Polymer Science, 101, 1362-1367, 2006.

[6] Jin Luo, Fumei Wang and Bugao Xu, Factors affecting crimp configuration of PTT/PET bicomponent filaments. Textile Research Journal, Vol. 81(5): 538-544, 2011.

[7] Lin Wenjing, Luo Jin, Wang Mei, Crimp and tensile properties of PTT/PET self-crimping staple fiber. Synthetic fiber (China), 1:27-31, 2010.

[8] Jin Luo, Guangbiao Xu, Fumei Wang, External configuration and crimp parameters of PTT/PET conjugated fiber, *Fibers and Polymers*, Vol.10, No.4, 508-512, 2009.

[9] Huvis Corp., Technical data of ESS PTT/PET bicomponent fibers, a private communication, 2007.

[10] Shi Meiwu, Crystal orientation structure and crimping properties of PET/PTT two-component elastic filament, Polymer Bulletin, 1: 37-44, 2009.

[11] DENTON M J., The crimp curvature of bi-component fibers. Journal of Textile Institute, 73(6):253-263, 1982.

[12] Sun Xunfang, Fang Xiaoshu, Guan Laitai, Mechanics of Materials, Higher Education Press, Beijing, China, 322-336, 2002.

[13] Shapiro, Linda G. and Stockman, George C., Computer Vision, Prentice-Hall, Inc., Upper Saddle River, New Jersey, USA, 2001.

AUTHORS' ADDRESSES

Fumei Wang, PhD
Fei Gu
College of Textiles, Donghua University
2999 North Renmin Road
Songjiang District
Shanghai 201620
CHINA

Bugao Xu, PhD
University of Texas
200 W 24th Street
Gearing Hall 225
Austin, Texas 78712
UNITED STATES